Intermittency and Persistence of Switching Modes in HfO_2-Based Memristors

E. Miranda, *Senior Member, IEEE*, A. Cantudo, F. Jiménez-Molinos, J. Suñé, *Fellow, IEEE*, M. B. González, and J. B. Roldán

***Abstract*— A distinct form of variability in HfO_2-based memristive devices is experimentally identified and analyzed. Unlike conventional cycle-to-cycle (C2C) variability, which is commonly associated with fluctuations within a single switching mechanism, the observed behaviour originates from the intermittent coexistence of well-distinguishable conduction modes. The devices exhibit spontaneous transitions between bipolar resistive switching (BRS) and complementary resistive switching (CRS), giving rise to persistent conduction states interrupted by abrupt mode changes. Statistical analysis based on the Wald-Wolfowitz runs test reveals statistically significant temporal correlations, indicating that the switching dynamics cannot be described as a purely random process. The voltage ramp rate is found to strongly influence the relative occurrence of both modes, progressively suppressing the CRS response until only the BRS mode remains observable at sufficiently high ramp rates. Numerical simulations based on the dynamic memdiode model reproduce the experimentally observed mode-switching behaviour and attribute its origin to the partial reconfiguration of the conductive filament. These results establish intermittency and persistence as key descriptors of conduction-mode variability in resistive switching dielectrics, revealing a form of variability that extends beyond conventional C2C fluctuations.**

***Index Terms*— Memristor, resistive switching, variability, persistence, intermittency, compact modeling.**

I. Introduction

MEMRISTIVE devices have attracted considerable attention for non-volatile memory, neuromorphic computing, and hardware security applications due to their scalable structure and programmable resistance states [1], [2]. Among the various switching mechanisms reported to date, filamentary resistive switching is one of the most extensively investigated because of its compatibility with CMOS technology and its potential for high-density integration [3]. However, the stochastic formation and rupture of conductive filaments give rise to cycle-to-cycle (C2C) variability, resulting in fluctuations of switching voltages and resistance states that remain a major challenge for reliable device operation [4], [5]. While C2C variability is commonly associated with fluctuations around a single switching mechanism, this work identifies a different form of variability arising from the coexistence of distinct conduction modes within the same device [6], [7], [8], [9], [10], [11], [12]. As shown in Fig. 1, the phenomenon manifests as an anomalous loop in the mean and median current-voltage (*I-V*) characteristics and originates from the random occurrence of two competing switching behaviors: conventional bipolar resistive switching (BRS) and complementary resistive switching (CRS). Systematic measurements, supported by lag-plot analysis, reveal that the competition between BRS and CRS modes is affected by the voltage ramp rate. As the sweep speed increases, the occurrence of the CRS mode progressively diminishes, eventually leaving BRS as the dominant switching mode at sufficiently high ramp rates.

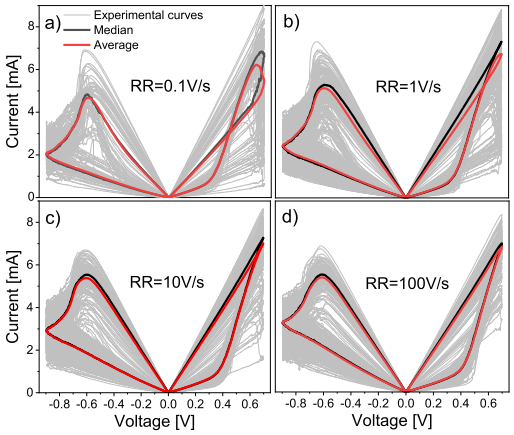


Fig. 1. Experimental *I-V* characteristics measured on the same device at different voltage ramp rates, with 215 switching cycles acquired for each ramp rate: a) *RR= 0.1* V/s, b) *RR= 1* V/s, c) *RR= 10* V/s and d) *RR= 100* V/s. The red and black solid lines correspond to the average and median *I-V* curves, respectively.

The objective of this work is to investigate the intermittent transitions between BRS and CRS modes in HfO_2-based memristive devices and to assess their temporal correlations

Received 25 July 2026; accepted 29 July 2026. Date of publication 6 August 2026; date of current version 29 September 2026. This work was supported by the Ministerio de Ciencia, Innovación y Universidades (MCIN)/Agencia Estatal de Investigación (AEI)/10.13039/501100011033 and Fondo Europeo de Desarrollo Regional (FEDER), European Union (EU), under Project PID2022-139586NB-C41, Project PID2022-139586NB-C42, and Project PID2022-139586NB-C44. The review of this letter was arranged by Editor X. Fong. *(Corresponding author: E. Miranda.)*

E. Miranda and J. Suñé are with Universitat Autònoma de Barcelona, 08193 Cerdanyola del Valles, Spain (e-mail: enrique.miranda@uab.cat).

A. Cantudo, F. Jiménez-Molinos, and J. B. Roldán are with the Universidad de Granada, 18071 Granada, Spain.

M. B. González is with the Institut de Microelectrònica de Barcelona, 08193 Cerdanyola del Valles, Spain.

Digital Object Identifier 10.1109/LED.2026.3719434

© 2026 The Authors. This work is licensed under a Creative Commons Attribution 4.0 License.
For more information, see https://creativecommons.org/licenses/by/4.0/

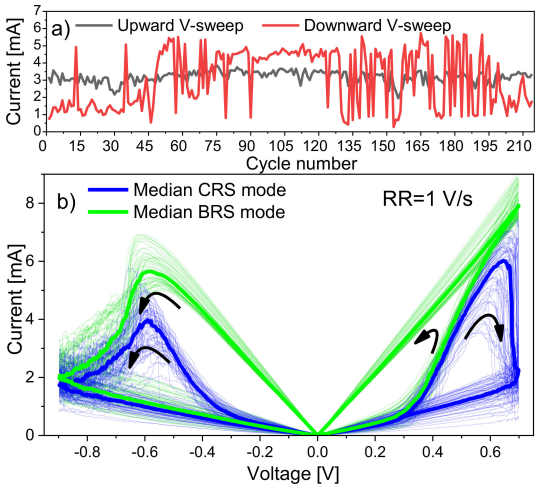


Fig. 2. a) Evolution of the current measured at 0.5 V for the upward and downward voltage sweeps as a function of the cycle number. b) Representative *I-V* characteristics extracted from Fig. 1a, illustrating the BRS and CRS modes investigated in this work.

using the Wald-Wolfowitz (WW) runs test [13], [14]. While intermittency describes the irregular alternation between distinct switching modes, persistence quantifies the degree of temporal correlation, *i.e.*, the extent to which the current state depends on previous switching events. To support the experimental findings and their interpretation, simulations based on the dynamic memdiode model (DMM) [15], [16], [17] are reported, reproducing the observed mode transition and attributing its origin to the partial reconfiguration of the conductive filament.

II. Devices and Measurements

The devices used in this work are conventional TiN(200 nm)/Ti(10 nm)/HfO_2(10 nm)/W(50 nm) RRAM cells. The HfO_2 films were deposited by atomic layer deposition (ALD) using tetrakis(dimethylamido)hafnium (TDMAH) as the hafnium precursor and water as the oxygen source. The metal electrodes were deposited by magnetron sputtering. The resulting structures consist of square cells with an area of $5\times5\,\mu m^2$. The devices were first electroformed. Measurements shown in this work correspond to single RRAM cells. As shown in Fig. 1, 215 switching cycles were performed for each voltage ramp rate (*RR* = 0.1, 1, 10, and 100 V/s). The applied voltage was swept between +0.7 V and −0.9 V without imposing a current compliance limit. Notice that the figure-eight-shaped hysteresis loop observed at low ramp rates progressively disappears with increasing ramp rate, leaving a conventional BRS response. Importantly, a 0.1 V increase in both the positive and negative voltage limits considered in Fig. 1, leads to complete stabilization of the conductive filament, thereby eliminating the CRS mode.

III. Statistical Analysis and Ramp Rate Effect

Figure 2a shows how the coexistence of competing conduction modes is reflected in the C2C evolution of the current. The black trace corresponds to the current measured at 0.5 V during the upward voltage sweep, whereas the red trace

RR[V/S]	N	R	↑%	TR[1/C]	E(R)	Z
0.1	213	65	51.17	0.302	107.4	-5.83
1	214	39	84.11	0.178	58.2	-4.94
10	214	15	92.52	0.066	30.61	-7.83
100	212	11	94.81	0.047	21.86	-7.75

Fig. 3. Comparative table of persistence and intermittency statistics across the four binary series investigated. *N* is the number of observations detected, *R* the number of runs, ↑% the state 1 percentage, *TR* the number of transitions per cycle, *E*(*R*) the number of runs expected for a completely random process, and *z* the asymptotic WW statistics.

corresponds to the current measured at the same voltage during the downward sweep. The intermittent crossing of both traces indicates repeated transitions between BRS and CRS modes. Representative *I-V* characteristics extracted from Fig. 1a are presented in Fig. 2b, highlighting the distinct electrical signatures associated with each mode. In addition to these mode transitions, conventional C2C variability is also present, contributing to the dispersion of the measured current levels [4]. To investigate the intermittency and persistence of this behaviour, the WW runs test was applied to current sequences such as that shown in Fig. 2a. The WW test is a non-parametric statistical method used to determine whether a sequence of events is randomly ordered or exhibits temporal correlations. It is based on the number of runs, *R*, defined as uninterrupted sequences of identical values, and compares the observed number of runs with that expected for a purely random sequence, *E*(*R*). Prior to the analysis, the current data were binarized using a threshold of 3.5 mA (see Fig. 2a), assigning a value of 0 to current values below the threshold and a value of 1 to those above it. The resulting binary sequences were subsequently analyzed to determine whether the alternation between conduction modes was consistent with a random process or instead exhibited statistically significant persistence, intermittency, and memory effects.

Across the four binary time series investigated, a clear gradient of persistence was observed (see Fig. 3). State 1 (BRS) frequency increased progressively from 51.17% (*RR= 0.1* V/s) through 84.11% (*RR= 1* V/s), 92.52% (*RR= 10* V/s), and 94.81% (*RR= 100* V/s). Correspondingly, the transition rate per cycle, *TR*, declined markedly from 0.302 (*RR= 0.1* V/s) to 0.047 (*RR= 100* V/s), indicating progressively lower intermittency. The maximum run length for state 1 increased substantially across series (33, 67, 120, and 120 consecutive observations, respectively), while maximum absence (state 0) runs remained comparatively short (21, 5, 7, and 5 observations). All four series departed significantly from randomness as confirmed by the WW runs test (asymptotic Z-statistics: $z = -5.83, -4.94, -7.83, -7.75$, all with p-value$\ll$ 1E-3), indicating systematic positive autocorrelation and state clustering in each case ($R < E(R)$, *i.e.* fewer runs than expected under randomness).

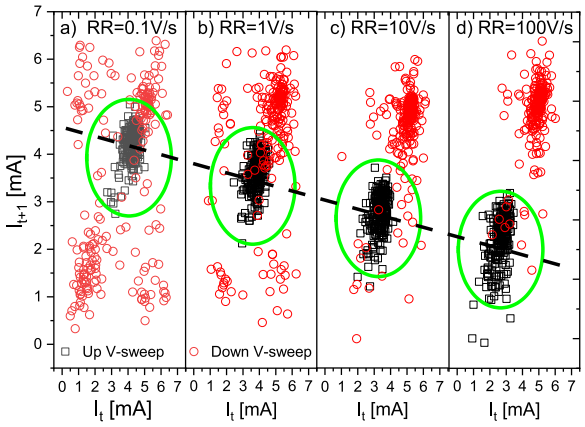


Fig. 4. Evolution of the lag plot (current measured at 0.5 V) as a function of *RR*. Black squares inside the green ellipses and red circles correspond to the upward and downward voltage sweeps, respectively. The dashed line is consistent with the set voltage shift.

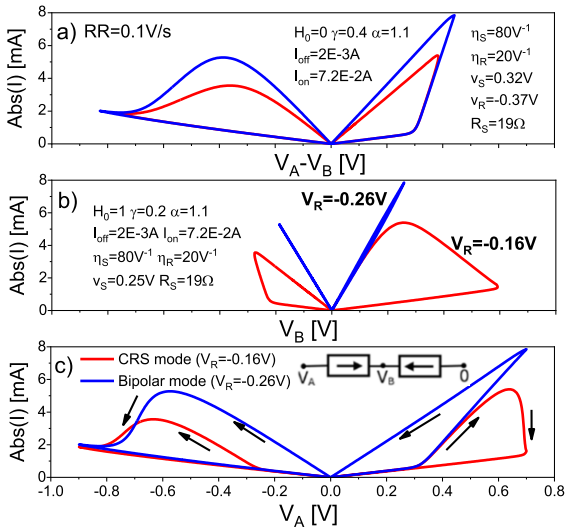


Fig. 5. a) and b), *I*-V characteristics of the switching elements before (red line) and after (blue line) the change in one of the model parameters. c) Combined action showing the CRS↔BRS transition. Voltage convention is indicated in the inset.

Lag plots were also employed as a complementary tool to visualize temporal correlations in the switching dynamics (see Fig. 4). By plotting the current measured in cycle $(i + 1)$ as a function of the current measured in cycle (i) at a fixed voltage (0.5 V), persistent conduction modes appear as clusters concentrated along the main diagonal of each plot, whereas intermittent transitions between modes generate off-diagonal populations. This representation provides direct visual evidence of the coexistence of BRS and CRS modes, as well as of the temporal correlations governing their evolution. As expected, the occurrence of the CRS mode (red circles below the black dashed line) progressively decreases with increasing *RR* and eventually disappears. This behavior is attributed to the shift of the device set voltage toward higher values at faster voltage sweeps [18], [19], which prevents the completion of the CRS cycle. These shifts are captured by the DMM [17].

IV. Model for the Switching I-V Characteristics

Based on the experimental observations discussed above, the coexistence of BRS and CRS modes can be interpreted as the result of different conductive filament configurations. Whereas BRS is associated with the response of a single memristive element, CRS can be viewed as the combined action of two oppositely biased memristive elements [20], [21], [22]. To simulate this behaviour, we employ the previously reported dynamic memdiode model (DMM), without any fundamental modification to its governing equations [17]. In this model, the electrical response emerges from the coupling between electron transport through the filament and voltage-driven vacancy migration, described by Eqs. (1) and (2), respectively:

$$I = \left[\left(I_{=on} - I_{off}\right) \cdot H + I_{off}\right] \cdot sinh\left(\alpha V_M\right) \tag{1}$$

$$\frac{dH}{dt} = e^{\eta_S (V_M - v_S)} \cdot (1 - H) - e^{-\eta_R H^V (V_M - v_R)} \cdot H \tag{2}$$

where $V_M = V\text{-}I \cdot R_S$. I_{on} and I_{off} denote the on and off-state currents of the memristor, respectively, α a fitting parameter, and R_S the series resistance [23], [24]. H is the memory state of the device. Parameters v_s and v_R correspond to the set and reset voltages, respectively, while η_s and η_R define the associated transition rates. γ is a smoothing parameter that controls the abruptness of the reset transition. Figures 5a and 5b show the individual responses of the two memristive elements forming the series configuration, plausibly originating from resistive switching processes occurring at or close to the two oxide/electrode interfaces [7]. The resulting behavior of the complete RRAM cell is shown in Fig. 5c. When both memristive elements are active their series combination gives rise to CRS behavior (red curves). This state, however, relies on a delicate balance between the switching parameters of the two elements. A small perturbation, such as for instance a 0.1 V shift in the reset voltage of one element (Fig. 5b), is sufficient to break this symmetry. Under these conditions, the perturbed element no longer contributes to the switching process and behaves approximately as a 30 Ω series resistor, suppressing the CRS response and yielding the BRS mode (blue curves). It should be emphasized that the DMM is a compact phenomenological model and does not attempt to explicitly describe the atomistic dynamics of filament formation and rupture. Instead, the inherent stochasticity of resistive switching is captured through variations in the model parameters associated with filament reconfiguration.

V. Conclusion

In summary, a distinct form of variability has been observed in HfO_2-based memristive devices, arising from intermittent transitions between switching modes. Statistical analysis demonstrates the presence of temporal correlations in the switching dynamics, while experiments reveal a strong dependence on voltage ramp rate. Simulations based on the dynamic memdiode model indicate that this behaviour can be explained by slight reconfigurations of the conductive filament driven by the inherently stochastic nature of resistive switching.

References

[1] L. Chua, "Resistance switching memories are memristors," *Appl. Phys. A, Solids Surf.*, vol. 102, no. 4, pp. 765–783, Mar. 2011, doi: 10.1007/s00339-011-6264-9.

[2] F. Aguirre, A. Sebastian, M. Le Gallo, W. Song, T. Wang, J. J. Yang, W. Lu, M.-F. Chang, D. Ielmini, Y. Yang, A. Mehonic, A. Kenyon, M. A. Villena, J. B. Roldán, Y. Wu, H.-H. Hsu, N. Raghavan, J. Suñé, E. Miranda, A. Eltawil, G. Setti, K. Smagulova, K. N. Salama, O. Krestinskaya, X. Yan, K.-W. Ang, S. Jain, S. Li, O. Alharbi, S. Pazos, and M. Lanza, "Hardware implementation of memristor-based artificial neural networks," *Nature Commun.*, vol. 15, no. 1, Mar. 2024, Art. no. 1974, doi: 10.1038/s41467-024-45670-9.

[3] S. Brivio, S. Spiga, and D. Ielmini, "HfO_2-based resistive switching memory devices for neuromorphic computing," *Neuromorphic Comput. Eng.*, vol. 2, no. 4, Dec. 2022, Art. no. 042001, doi: 10.1088/2634-4386/ac9012.

[4] J. B. Roldán, E. Miranda, D. Maldonado, A. N. Mikhaylov, N. V. Agudov, A. A. Dubkov, M. N. Koryazhkina, M. B. González, M. A. Villena, S. Poblador, M. Saludes-Tapia, R. Picos, F. Jiménez-Molinos, S. G. Stavrinides, E. Salvador, F. J. Alonso, F. Campabadal, B. Spagnolo, M. Lanza, and L. O. Chua, "Variability in resistive memories," *Adv. Intell. Syst.*, vol. 5, no. 6, Jun. 2023, Art. no. 2200338, doi: 10.1002/aisy.202200338.

[5] W. Sun, B. Gao, M. Chi, Q. Xia, J. J. Yang, H. Qian, and H. Wu, "Understanding memristive switching via in situ characterization and device modeling," *Nature Commun.*, vol. 10, no. 1, Aug. 2019, Art. no. 3453, doi: 10.1038/s41467-019-11411-6.

[6] Y. Yang, P. Sheridan, and W. Lu, "Complementary resistive switching in tantalum oxide-based resistive memory devices," *Appl. Phys. Lett.*, vol. 100, no. 20, May 2012, Art. no. 203112, doi: 10.1063/1.4719198.

[7] D.-H. Lim, G.-Y. Kim, J.-H. Song, K.-S. Jeong, D.-H. Ko, and M.-H. Cho, "Filament geometry induced bipolar, complementary and unipolar resistive switching under the same set current compliance in Pt/SiO_x/TiN," *Sci. Rep.*, vol. 5, no. 1, Oct. 2015, Art. no. 15374, doi: 10.1038/srep15374.

[8] X. Qiu, H. Gao, S. Zhu, Y. Bai, Y. Zhao, R. Wang, X. Ma, and Y. Yang, "Bipolar and complementary resistive switching induced by barrier regulation based on compliance current," *Appl. Phys. Lett.*, vol. 124, no. 23, Jun. 2024, Art. no. 233509, doi: 10.1063/5.0208867.

[9] S. Petzold, E. Miranda, S. U. Sharath, J. Muñoz-Gorriz, T. Vogel, E. Piros, N. Kaiser, R. Eilhardt, A. Zintler, L. Molina-Luna, J. Suñé, and L. Alff, "Analysis and simulation of the multiple resistive switching modes occurring in HfOx-based resistive random access memories using memdiodes," *J. Appl. Phys.*, vol. 125, no. 23, Jun. 2019, Art. no. 234503, doi: 10.1063/1.5094864.

[10] V. R. Nallagatla, J. Kim, K. Lee, S. C. Chae, C. S. Hwang, and C. U. Jung, "Complementary resistive switching and synaptic-like memory behavior in an epitaxial $SrFeO_{2.5}$ thin film through oriented oxygen-vacancy channels," *ACS Appl. Mater. Interface*, vol. 12, no. 37, pp. 41740–41748, Sep. 2020, doi: 10.1021/acsami.0c10910.

[11] S. Sarkar, F. Y. Rahman, H. Banik, S. Majumdar, D. Bhattacharjee, and S. A. Hussain, "Complementary resistive switching behavior in tetraindolyl derivative-based memory devices," *Langmuir*, vol. 38, no. 30, pp. 9229–9238, Aug. 2022, doi: 10.1021/acs.langmuir.2c01011.

[12] G. Kim, J. Sung, S. Kang, J. Lim, and C. Shin, "Investigation of the switching mechanism in the bipolar and complementary resistive switching of HfO_x-based resistive random-access memory through rapid-thermal-annealing-induced grain boundary engineering," *ACS Appl. Electron. Mater.*, vol. 7, no. 8, pp. 3561–3570, Apr. 2025, doi: 10.1021/acsaelm.5c00344.

[13] A. Wald and J. Wolfowitz, "On a test whether two samples are from the same population," *Ann. Math. Statist.*, vol. 11, no. 2, pp. 147–162, Jun. 1940, doi: 10.1214/aoms/1177731909.

[14] J. M. D. L. Rubia, "Calculation of two-tailed exact probability in the Wald–Wolfowitz one-sample runs test," *J. Data Anal. Inf. Process.*, vol. 12, no. 1, pp. 89–114, 2024, doi: 10.4236/jdaip.2024.121006.

[15] E. Miranda, "Compact model for the major and minor hysteretic I–V loops in nonlinear memristive devices," *IEEE Trans. Nanotechnol.*, vol. 14, no. 5, pp. 787–789, Sep. 2015, doi: 10.1109/TNANO.2015.2455235.

[16] F.L. Aguirre, S. Pazos, F. Palumbo, J. Suñé, and E. Miranda, "Application of the quasi-static memdiode model in cross-point arrays for large dataset pattern recognition," *IEEE Access*, vol. 8, pp. 202174–202193, 2020, doi: 10.1109/ACCESS.2020.3035638.

[17] F. L. Aguirre, J. Suñé, and E. Miranda, "SPICE implementation of the dynamic memdiode model for bipolar resistive switching devices," *Micromachines*, vol. 13, no. 2, p. 330, Feb. 2022, doi: 10.3390/mi13020330.

[18] M. Maestro-Izquierdo, M. B. Gonzalez, F. Campabadal, J. Sune, and E. Miranda, "A new perspective towards the understanding of the frequency-dependent behavior of memristive devices," *IEEE Electron Device Lett.*, vol. 42, no. 4, pp. 565–568, Apr. 2021, doi: 10.1109/LED.2021.3063239.

[19] H. García, G. Vinuesa, E. García-Ochoa, F. L. Aguirre, M. B. González, F. Jiménez-Molinos, F. Campabadal, J. B. Roldán, E. Miranda, S. Dueñas, and H. Castán, "Effects of the voltage ramp rate on the conduction characteristics of HfO2-based resistive switching devices," *J. Phys. D, Appl. Phys.*, vol. 56, no. 36, Sep. 2023, Art. no. 365108, doi: 10.1088/1361-6463/acdae0.

[20] E. Linn, R. Rosezin, C. Kügeler, and R. Waser, "Complementary resistive switches for passive nanocrossbar memories," *Nature Mater*, vol. 9, pp. 403–406, May 2010, doi: 10.1038/nmat2748.

[21] M. Saludes-Tapia, S. Poblador, M. B. Gonzalez, F. Campabadal, J. Suñe, and E. Miranda, "Tunability properties and compact modeling of HfO_2-based complementary resistive switches using a three-terminal subcircuit," *IEEE Trans. Electron Devices*, vol. 68, no. 12, pp. 5981–5988, Dec. 2021, doi: 10.1109/TED.2021.3117488.

[22] M. Saludes-Tapia, S. Poblador, F. Campabadal, J. Suñe, M. B. González, and E. Miranda, "Electrical characterization and compact modeling of HfO_2-based complementary resistive switching devices," in *Nonvolatile Memory and Selector Devices*, W. Banerjee, Ed., Hoboken, NJ, USA: Wiley, 2026, doi: 10.1002/9783527847419.

[23] M. B. Gonzalez, M. Maestro-Izquierdo, F. Jiménez-Molinos, J. B. Roldán, and F. Campabadal, "Current transient response and role of the internal resistance in HfO_x-based memristors," *Appl. Phys. Lett.*, vol. 117, no. 26, Dec. 2020, Art. no. 262902, doi: 10.1063/5.0031575.

[24] D. Maldonado, F. Aguirre, G. González-Cordero, A. M. Roldán, M. B. González, F. Jiménez-Molinos, F. Campabadal, E. Miranda, and J. B. Roldán, "Experimental study of the series resistance effect and its impact on the compact modeling of the conduction characteristics of HfO_2-based resistive switching memories," *J. Appl. Phys.*, vol. 130, no. 5, Aug. 2021, Art. no. 054503, doi: 10.1063/5.0055982.